Available online at www.sciencedirect.com
ScienceDirect
Bioorganic & Medicinal Chemistry Letters 17 (2007) 6192–6196
Bioorganic & Medicinal Chemistry Letters

# Peptidomimetic inhibitors of farnesyltransferase with high in vitro activity and significant cellular potency

Cristiano Bolchi,[a] Marco Pallavicini,[a] Chiara Rusconi,[a] Luisa Diomede,[b] Nicola Ferri,[c] Alberto Corsini,[c] Laura Fumagalli,[a] Alessandro Pedretti,[a] Giulio Vistoli[a] and Ermanno Valoti[a,*]

[a]*Istituto di Chimica Farmaceutica e Tossicologica ''Pietro Pratesi'', Università di Milano, via Mangiagalli 25, I-20133 Milano, Italy*
[b]*Dipartimento di Biochimica e Farmacologia Molecolare, Istituto di Ricerche Farmacologiche ''Mario Negri'', via La Masa 19, I-20156 Milano, Italy*
[c]*Dipartimento di Scienze Farmacologiche, Università di Milano, via Balzaretti 9, I-20133 Milano, Italy*

Received 30 July 2007; revised 5 September 2007; accepted 5 September 2007
Available online 8 September 2007

Dedicated to Professor Luigi Villa in memory of his outstanding teaching and research contribution.

**Abstract**—2-*o*-Tolyl or 2-*o*-anisyl substituted 4-hydroxy- and 4-carboxybenzamides of methionine, etherified and amidified with 2-hydroxymethyl- and 2-aminomethylpyridodioxane, respectively, are described as inhibitors of Ras protein farnesyltransferase (FTase). Of the sixteen compounds, resulting from the substitution pattern of benzamide and the configuration of the two stereocenters, seven inhibited FTase activity with potencies in the nanomolar range. They were all 2-oxymethylpyridodioxane ethers and, among them, the four *o*-tolyl substituted stereoisomers also showed micromolar antiproliferative effect on human aortic smooth muscle cells interfering with Ras farnesylation. The docking analysis enlightened significant differences in enzyme interaction between oxymethylpyridodioxane and aminomethylpyridodioxane derivatives.


Farnesyltransferase enzyme (FTase) catalyzes the covalent transfer of the isoprenoid farnesyl from prenyl donor farnesyldiphosphate (FPP) to a cysteine residue of protein substrates, such as Ras proteins, containing a C-terminal *CAAX* motif, in which *C* is the cysteine that is farnesylated, *AA* are usually aliphatic aminoacids, and *X* is the terminal aminoacid, normally methionine, serine, alanine, or glutamine. Prenylation of Ras proteins by FTase is essential for these proteins to take part in the transduction of extracellular mitogenic signals to the nucleus. Because mutant Ras proteins are responsible for about 30% of all human cancers and their malignant activity is also dependent on FTase catalyzed prenylation, farnesyltransferase inhibitors (FTIs) have emerged as a new class of extremely promising anticancer drugs.[1] More recently, FTIs have been thought to be effective in preventing proliferation of smooth muscle cells (SMCs) in the arterial wall,[2,3] a prominent feature of atherosclerosis and restenosis after angioplasty and coronary stent implantation.[4] Finally, FTIs that specifically target FTases of protozoan parasites, such as *Plasmodium falciparum* or *Trypanosome brucei*, have been proposed for the treatment of parasitic infections.[5–10]

The discovery that *CAAX* tetrapeptides can potently inhibit FTase in cell-free assays,[11,12] though totally inactive in whole cells, has prompted the development of *CAAX* mimetics with progressively minimized peptidic features in order to obtain FTIs with higher metabolic stability and improved cell permeability. These objectives were achieved through modifications such as (a) the isosteric replacement of the internal dipeptide (*AA*) with 4-amino or 4-hydroxy substituted 2-biphenylcarboxylic acid and the *ortho* methylation or methoxylation of the flanking phenyl ring of the biphenyl spacer and (b) the replacement of the cysteine residue (*C*), bearing the problematic thiol group, by 3-pyridyl, optimally linked to the biphenyl core by an oxymethylene bridge.[13–15]

Based on such observations, we designed the structures **1**–**16**, whose salient feature is the presence of pyridodioxane in lieu of 3-pyridyl ether to mimic the cysteine

*Keywords*: Farnesyltransferase; Peptidomimetic inhibitors; Antiproliferative agents; Antitumors.
* Corresponding author. E-mail: ermanno.valoti@unimi.it

0960-894X/$ - see front matter © 2007 Elsevier Ltd. All rights reserved.
doi:10.1016/j.bmcl.2007.09.015

residue of *CAAX* tetrapeptides. The replacement was undertaken in order to restrict the conformational freedom of this portion of the molecules, while improving its hydrogen bond acceptor capability, thanks to the additional oxygen, and making it chiral by the presence of the novel dioxane stereocenter.

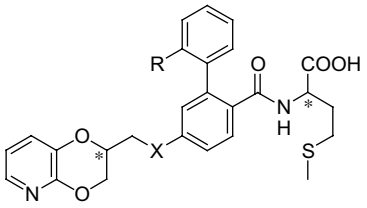

**1-4** R = Me X = O
**5-8** = OMe = O
**9-12** = Me = NHCO
**13-16** = OMe = NHCO

The synthetic accessibility to the pyridodioxane synthon as unichiral 2-hydroxymethyl and 2-aminomethyl derivatives led us to conceive its connection to the biphenyl core through a short methyleneoxy and methyleneaminocarbonyl chain, respectively.

To synthesize compounds **1**–**8**, we firstly prepared the two non-aminoacidic building blocks, namely the mesyloxymethylpyridodioxane **18**, in both the enantiomeric forms, and ethyl 4-hydroxybenzoate, *o*-tolyl or *o*-anisyl substituted at position 2 (**27** and **28**, respectively).

As outlined in Scheme 1, the *R* enantiomer of intermediate **18** was obtained by mesylation of (*S*)-2-hydroxymethyl-2,3-dihydro[1,4]dioxino-[2,3-*b*]pyridine (*S*)-**17**, whose univocal synthesis from (*S*)-benzylglycerol we have recently reported together with that of its antipode from (*R*)-benzylglycerol.[16] Analogously, (*R*)-**17** was transformed into mesylate (*S*)-**18**.

As shown in Scheme 2, compound **27** was prepared from 2-bromo-4-nitrobenzoic acid **21**,[17] which was converted into ethyl ester **22** and then coupled with tolyl boronic acid using Suzuki conditions to give biphenyl derivative **23**. Successive reduction of nitro to amino group afforded **25**, which was submitted to diazotation and diazonium salt decomposition yielding ethyl 2-(2-methylphenyl)-4-hydroxybenzoate **27**. The same synthetic

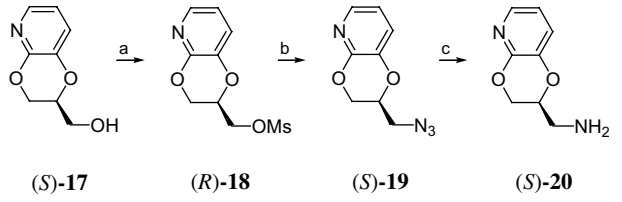

(*S*)-**17** (*R*)-**18** (*S*)-**19** (*S*)-**20**

**Scheme 1.** Synthesis of the *S* enantiomer of aminomethylpyridodioxane. Reagents and conditions: (a) MsCl, TEA, DCM, rt, 1 h, 98%; (b) $NaN_3$, DMF, $H_2O$, reflux, 6 h, 91%; (c) $N_2H_4$, PdO, MeOH, reflux, 2 h, 92%.

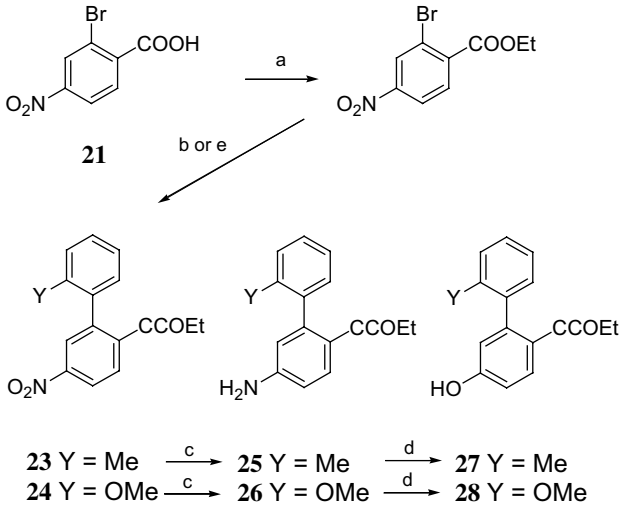

**Scheme 2.** Synthesis of the ethyl esters of 2-*o*-tolyl- and 2-*o*-anisyl-4-hydroxybenzoic acid. Reagents and conditions: (a) ethanol, ethyl orthoformate, $H_2SO_4$ concd, reflux, 12 h, 79%; (b) tolyl boronic acid, $Pd(PPh_3)_4$, 2 M $Na_2CO_3$, ethanol, toluene, reflux, 12 h, 90%; (c) $H_2$-Pd/C, methanol, 3 h, 73% (**25**) and 86% (**26**); (d) $NaNO_2$, 2 N $H_2SO_4$, acetone, −10 °C and then rt, 12 h, 91% (**27**) and 89% (**28**); (e) *o*-methoxyphenyl boronic acid, $Pd(PPh_3)_4$, 2 M $Na_2CO_3$, ethanol, toluene, reflux, 12 h, 81%.

sequence led to ethyl 2-(2-methoxyphenyl)-4-hydroxybenzoate **28** starting from **21**, but using *o*-methoxyphenyl boronic acid in place of tolyl boronic acid (Scheme 2).

Nucleophilic displacement of mesylate group of (*R*)-**18** by the sodium salts of **27** and **28** yielded (*S*)-**32** and (*S*)-**33**, respectively. Both these ethyl esters were hydrolyzed and the resultant carboxylic acids (*S*)-**34** and (*S*)-**35** condensed with L-methionine methyl ester to give the corresponding amides **36** and **37**, whose ester function was hydrolyzed yielding the target compounds **1** and **5** with *S* configuration at both the stereocenters (Scheme 3). The corresponding *RR* enantiomers **2** and **6** were synthesized from (*S*)-**18** and D-methionine methyl ester by the same sequence of reactions illustrated in Scheme 3. Identically, the stereoisomers **3** and **7**, having the benzodioxane stereocenter in *S* configuration and the aminoacid residue in *R* configuration, and the respective enantiomers **4** and **8** were prepared using (*R*)-**18** and D-methionine methyl ester in the former case and (*S*)-**18** and L-methionine methyl ester in the latter.

The synthesis of compounds **9**–**16** required unichiral aminomethylpyridodioxane **20**, readily accessible in both the enantiomeric forms from (*R*)-**18** and (*S*)-**18** (see Scheme 1 for (*S*)-**20**) and, as a biphenyl derivative, methyl 2-(2-methylphenyl)-4-carboxybenzoate[18] or its methoxy analogue **31**, which was prepared from commercially available dimethyl 2-iodoterephthalate **29** as shown in Scheme 4. To prepare **9** and **13**, these two methyl carboxybenzoates were reacted with (*S*)-**20** obtaining (*S*)-**44** and (*S*)-**45**, respectively (Scheme 5). Successive hydrolysis of methyl ester afforded the carboxylic acids (*S*)-**46** and (*S*)-**47**, which were condensed with L-methionine methyl ester to give **48** and **49**, respec-

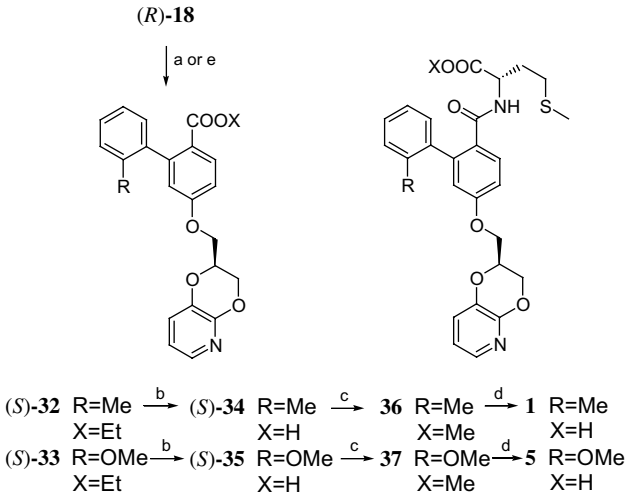


**Scheme 3.** Synthesis of compounds **1** and **5**. Reagents and conditions: (a) **27**, NaH, DME, −15 °C and then reflux, 48 h, 56%; (b) 3 N KOH, methanol, 50 °C, 12 h, 86% ((*S*)-**34**) and 70% ((*S*)-**35**); (c) L-methionine methyl ester hydrochloride, HOBt, EDAC, DMF, 15 min, rt and then TEA, 24 h, rt, 69% (**36**) and 72% (**37**); (d) 3 N KOH, methanol, 12 h, rt, 92% (**1**) and 91% (**5**); (e) **28**, NaH, DME, −15 °C and then reflux, 48 h, 86%.

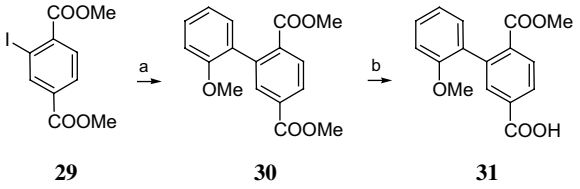


**Scheme 4.** Synthesis of compound **31**. Reagents and conditions: (a) *o*-methoxyphenyl boronic acid, $Pd(PPh_3)_4$, 2 M $Na_2CO_3$, ethanol, toluene, reflux, 3 h, 75%; (b) 1.7 N KOH, 1/1 THF/methanol, rt, 12 h, 72%.

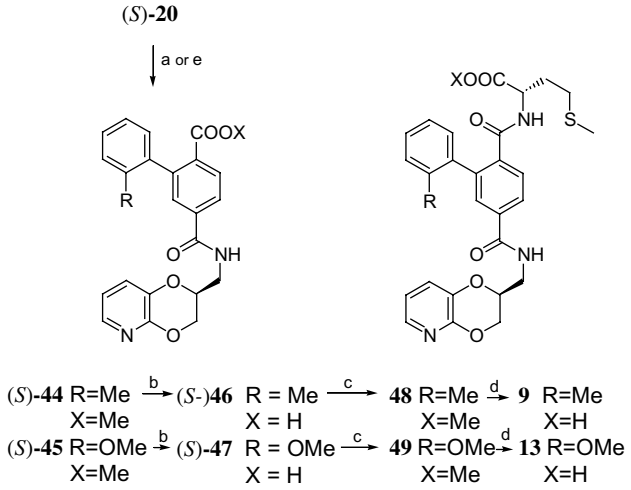


**Scheme 5.** Synthesis of compounds **9** and **13**. Reagents and conditions: (a) methyl 2-*o*-tolyl-4-carboxybenzoate, HOBt, EDAC, DMF, 15 min, rt and then TEA, 12 h, rt, 63%; (b) 3 N KOH, methanol, 4 h, rt, 95% ((*S*)-**46**) and 96% ((*S*)-**47**); (c) L-methionine methyl ester hydrochloride, HOBt, EDAC, DMF, 15 min, rt and then TEA, 24 h, rt, 64%; (d) 3 N KOH, methanol, 12 h, rt, 96% (**9**) and 91% (**13**); (e) **31**, HOBt, EDAC, DMF, 15 min, rt and then TEA, 12 h, rt, 65%.

tively. Finally, the methionine ester function was hydrolyzed yielding the target compounds **9** and **13** with *S* configuration at both the stereocenters. The same synthetic route shown in Scheme 5 was followed to prepare the corresponding *RR* enantiomers **10** and **14**, the stereoisomers **11** and **15**, with *S* and *R* configuration at pyridodioxane and methionine stereocenter, respectively, and the enantiomers of these latter **12** and **16** using aminomethylpyridodioxane **20** and methionine methyl ester in the required configuration.

Initially, compounds **1**–**16** were tested for their ability to inhibit FTase activity and the respective $IC_{50}$ values are listed in Table 1. Successively, the same compounds were examined in a cellular assay that measured inhibition of human aortic SMC proliferation. The most active FTase inhibitors, namely the *o*-methylated biphenyl ethers **1**–**4**, efficiently inhibited SMC proliferation in a concentration dependent manner with an $IC_{50}$ value in the micromolar range (Table 2), whereas the other compounds did not show any significant effect at concentrations ranging from 50 to 250 μM.

To directly evaluate the effect of the compounds with antiproliferative activity, in particular of **2** and **4**, on protein prenylation, Ras farnesylation process was

**Table 1.** Inhibition of FTase activity and interaction energies with FTase of compounds **1**–**16** (in brackets the absolute configuration of methionine residue and then that of the pyridodioxanemethyl substituent)

| Compound | $IC_{50}$ (μM) | Energy (kcal/mol) |
|---|---|---|
| **1** (*SS*) | 0.050 | −55.15 |
| **2** (*RR*) | 0.053 | −55.04 |
| **3** (*RS*) | 0.075 | −57.62 |
| **4** (*SR*) | 0.045 | −58.02 |
| **5** (*SS*) | 0.053 | −53.38 |
| **6** (*RR*) | 0.112 | −53.56 |
| **7** (*RS*) | >1000 | −54.60 |
| **8** (*SR*) | 0.055 | −58.48 |
| **9** (*SS*) | 12 | −37.61 |
| **10** (*RR*) | >1000 | −49.24 |
| **11** (*RS*) | >1000 | −43.83 |
| **12** (*SR*) | 16 | −38.69 |
| **13** (*SS*) | 302 | −52.81 |
| **14** (*RR*) | >1000 | −52.24 |
| **15** (*RS*) | 843 | −44.52 |
| **16** (*SR*) | 151 | −52.83 |

The inhibition curves were fitted using 'one-site competition' equation built into Prism version 4.0 for Windows (GraphPad Software, San Diego, CA). This analysis gives the $IC_{50}$ (the drug concentration inhibiting the enzyme activity by 50%) with a 95% of confidence interval. The energy values were obtained by molecular docking calculation.

**Table 2.** Antiproliferative effect of compounds **1**–**4** on human aortic SMCs

| Compound | **1** | **2** | **3** | **4** |
|---|---|---|---|---|
| $IC_{50}$ (μM) | 157.9 | 16.8 | 237.8 | 58.8 |

The $IC_{50}$ values were determined by linear regression analysis of the logarithm of the concentration versus the percentage of the inhibitory effect.

estimated by Western blot analysis from a total protein extract of cells incubated under the same experimental conditions utilized for evaluating cell proliferation.

Compounds **2** and **4**, at 250 μM, proved to directly interfere with Ras farnesylation as indicated by the appearance of a slower migrating band also after incubation with HMG-CoA reductase inhibitor simvastatin (Fig. 1).

Compounds **1**–**16** were docked in the crystal structure of human FTase. The resultant inhibitor–enzyme interaction energies are reported in Table 1. It is significant that the phenyl ethers **1**–**8**, all much more potent FTIs, with the exception of **7**, than the benzamides **9**–**16**, show lower interaction energies than these latter occupying the first eight positions in the energy rank. Furthermore, the *o*-methyl substituted compounds **1**–**4**, the most potent inhibitors of FTase and of cell proliferation in the series, are also the top interacting ones in terms of energy.

The configuration of the two stereocenters does not exert significant influence on the activity of these compounds. Excepting **7**, all the enantiomers and the diastereomers are virtually equiactive in the series of the most active phenyl ethers **1**–**8** and this is consistent with the modest energy differences resulting from molecular docking. On the contrary, molecular docking enlightens the importance of the linker between biphenyl core and pyridodioxane for the role played by the biheterocycle in the interaction with the enzyme. In the FTase complexes with methyleneoxy compounds **1**–**8**, the pyridodioxane system shields the enzyme zinc ion, which is conversely engaged in an ionic interaction with the methionine carboxyl of the inhibitor in the FTase complexes with methyleneaminocarbonyl compounds **9**–**16** (Fig. 2). Such a different binding mode could explain the great difference in FTase inhibiting activity between the phenylethers **1**–**8** and the benzamides **9**–**16**.

In conclusion, we have demonstrated that *CAAX* mimetics, in which cysteine is replaced by a pyridodioxanemethyl residue etherifying the known *AA* bioisostere 2-*o*-tolyl-4-hydroxybenzoic acid, inhibit FTase activity both in cell-free and in whole cell tests at nanomolar and micromolar level, respectively. Consistently with docking results, critical features of such new FTIs are the nature of the short linker between pyridodioxane and biphenyl core and the *o*-substitution on this latter, and not the configuration of the two stereocenters.

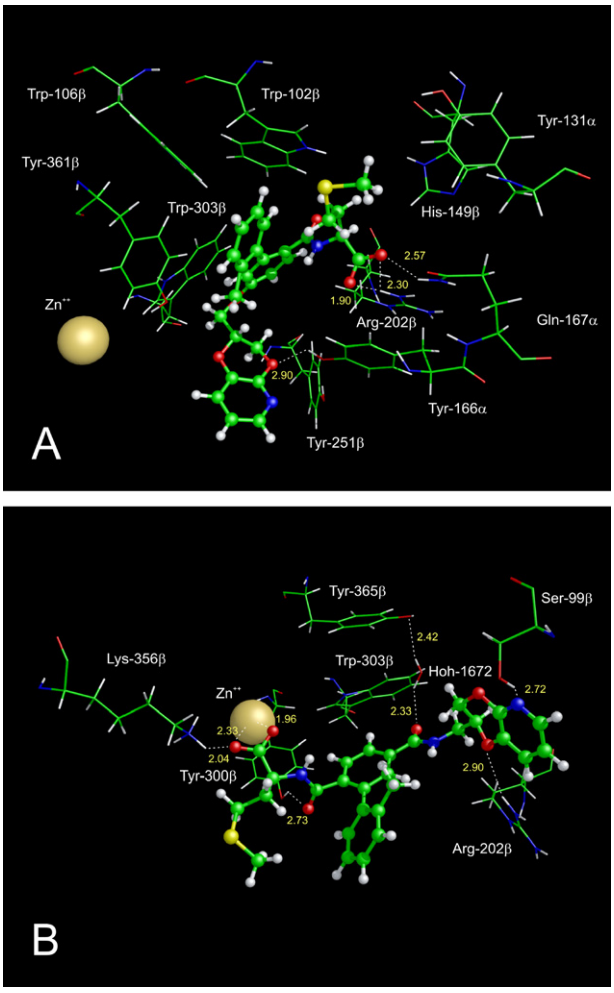


**Figure 2.** Complexes of the human FTase with **4** (A) and **9** (B) showing the two different binding modes typical of oxymethylpyridodioxane ethers **1**–**8** and aminomethylpyridodioxane amides **9**–**16**. In the former (A), the ligand is placed in a hydrophobic pocket lined by several aromatic residues of both α and β FTase subunits and the carboxyl group interacts with the Arg-202β and the Gln-167α residues. In the latter (B), the main interactions involve the residues of the β subunit and the ligand carboxyl group interacts with the zinc ion.

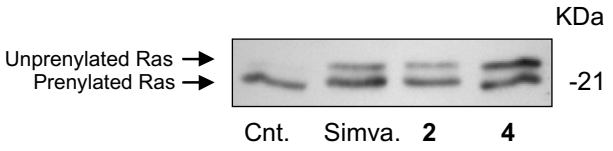


**Figure 1.** Experimental conditions are as in Table 2. After 72 h incubation of the cells with 250 μM concentration of compounds **2** and **4** and 2 μM simvastatin (Simva), total cell lysates were prepared and Ras prenylation evaluated by Western blotting analysis with a specific antibody (anti Ras clone, Upstate). The slower migrating band represents the unprenylated form of Ras (Unpre. Ras), while the faster migrating band is prenylated Ras (Pre. Ras).

## Acknowledgment

Financial support provided by the Italian Ministero dell'Istruzione, dell'Università e della Ricerca Scientifica is gratefully acknowledged.

## Supplementary data

Supplementary data associated with this article can be found, in the online version, at doi:10.1016/j.bmcl.2007.09.015.

## References and notes


1. Basso, A. D.; Kirschmeier, P.; Bishop, W. R. *J. Lipid Res.* **2006**, *47*, 15.
2. Indolfi, C.; Avvedimento, E. V.; Rapacciuolo, A.; Di Lorenzo, E.; Esposito, G.; Stabile, E.; Feliciello, A.; Mele, E.; Giuliano, P.; Condorelli, G.; Chiariello, M. *Nat. Med.* **1995**, *1*, 541.
3. Work, L. M.; McPhaden, A. R.; Pyne, N. J.; Pyne, S.; Wadsworth, R. M.; Wainwright, C. L. *Circulation* **2001**, *104*, 1538.
4. Kipshidze, N. N.; Tsapenko, M. V.; Leon, M. B.; Stone, G. W.; Moses, J. W. *Exp. Rev. Cardiovasc. Ther.* **2005**, *3*, 953.
5. Yokoyama, K.; Trobridge, P.; Buckner, F. S.; Van Voorhis, W. C.; Stuart, K. D.; Gelb, M. H. *J. Biol. Chem.* **1998**, *273*, 26497.
6. Yokoyama, K.; Trobridge, P.; Buckner, F. S.; Sholten, J.; Stuart, K. D.; Van Voorhis, W. C.; Gelb, M. H. *Mol. Biochem. Parasitol.* **1998**, *94*, 87.
7. Couto, A. S.; Rimura, E. A.; Peres, V. J.; Uhrig, M. L.; Katzin, A. M. *Biochem. J.* **1999**, *341*, 629.
8. Chakrabarti, D.; Azam, T.; DelVecchio, C.; Qiu, L.; Park, Y.; Allen, C. M. *Mol. Biochem. Parasitol.* **1998**, *94*, 175.
9. Wiesner, J.; Kettler, K.; Sakowski, J.; Ortmann, R.; Katzin, A. M.; Rimura, E. A.; Silber, K.; Klebe, G.; Jomaa, H.; Schlitzer, M. *Angew. Chem. Int. Ed.* **2004**, *43*, 251.
10. Nallan, L.; Bauer, K. D.; Bendale, P.; Rivas, K.; Yokoyama, K.; Hornéy, C. P.; Pendyala, P. R.; Floyd, D.; Lombardo, L. J.; Williams, D. K.; Hamilton, A.; Sebti, S.; Windsor, W. T.; Weber, P. C.; Buckner, F. S.; Chakrabarti, D.; Gelb, M. H.; Van Voorhis, W. C. *J. Med. Chem.* **2005**, *48*, 3704.
11. Goldstein, J. L.; Brown, M. S.; Stradley, S. T.; Reiss, Y.; Gierasch, L. M. *J. Biol. Chem.* **1991**, *266*, 15575.
12. Reiss, Y.; Stradley, S.; Gierasch, L.; Brown, M. S.; Goldstein, J. L. *Proc. Natl. Acad. Sci. U.S.A.* **1991**, *88*, 732.
13. Sun, J.; Qian, Y.; Hamilton, A. D.; Sebti, S. M. *Cancer Res.* **1995**, *55*, 4243.
14. Qian, Y.; Vogt, A.; Sebti, S. M.; Hamilton, A. D. *J. Med. Chem.* **1996**, *39*, 217.
15. Augeri, D. J.; O'Connor, S. J.; Janowick, D.; Szczepankiewicz, B.; Sullivan, G.; Larsen, J.; Kalvin, D.; Cohen, J.; Devine, E.; Zhang, H.; Cherian, S.; Saeed, B.; Ng, S. C.; Rosenberg, S. *J. Med. Chem.* **1998**, *41*, 4288.
16. Bolchi, C.; Pallavicini, M.; Fumagalli, L.; Moroni, B.; Rusconi, C.; Valoti, E. *Tetrahedron: Asymmetry* **2005**, *16*, 3380.
17. Carrico, D.; Ohkanda, J.; Kendrick, H.; Yokoyama, K.; Blaskovich, M. A.; Bucher, C. J.; Buckner, F. S.; Van Voorhis, W. C.; Chakrabarti, D.; Croft, S. L.; Gelb, M. H.; Sebti, S. M.; Hamilton, A. D. *Bioorg. Med. Chem.* **2004**, *12*, 6517.
18. Sebti, S. M.; Hamilton, A. D.; Augeri, D. J.; Barr, K. J.; Donner, J. B.; Fakhoury, S. A.; O'Connor, S. J.; Rosenberg, S. H.; Shen, W.; Szczepankiewicz, B. G. U.S. Patent 2002193596, 2002; *Chem. Abstr.* **2002**, *138*, 39539.